

9-Nitroanthracene derivative as a precursor of anthraquinone for photodynamic therapy

Kiyoshi Fukuhara,^{a,*} Shinji Oikawa,^b Nana Hakoda,^b Yasunori Sakai,^c Yusuke Hiraku,^b Takuji Shoda,^a Shinichi Saito,^c Naoki Miyata,^d Shosuke Kawanishi^{b,e} and Haruhiro Okuda^a

^aDivision of Organic Chemistry, National Institute of Health Sciences, 1-18-1 Setagaya-ku, Tokyo 158-8501, Japan

^bDepartment of Environmental and Molecular Medicine, Mie University Graduate School of Medicine, Tsu, Mie 514-8507, Japan

^cFaculty of Science, Tokyo University of Science, Shinjuku-ku, Tokyo 162-8601, Japan

^dGraduate School of Pharmaceutical Sciences, Nagoya City University, Mizuho-ku, Nagoya, Aichi 467-8603, Japan

^eFaculty of Health Science, Suzuka University of Medical Science, Suzuka, Mie 510-0293, Japan

Received 29 January 2007; revised 6 March 2007; accepted 7 March 2007

Available online 13 March 2007

Abstract—Anthraquinones are typical photosensitizers used in photodynamic therapy (PDT). However, systemic toxicity is a major problem for anthraquinones due to their ability not only to bind DNA but also to cause oxidative stress even without photoirradiation. To avoid such disadvantages in cancer therapy, we designed and synthesized a novel 9-nitroanthracene derivative (**1**) as a precursor of anthraquinone. Under photoirradiation, **1** is converted into anthraquinone via generation of nitric oxide as confirmed by ESR. Strong DNA cleavage specifically at guanine under photoirradiation was also observed, characteristic of DNA-cleaving reactions by photoirradiated anthraquinones. We propose development of **1** as an alternative approach toward PDT that reduces the systemic toxicity of anthraquinone.

© 2007 Elsevier Ltd. All rights reserved.

1. Introduction

Photodynamic therapy (PDT) is an attractive approach to selectively localize toxicity using photosensitizers activated by light to induce cell death.^{1,2} A large number of porphyrins have been tested for their efficacy in PDT, photofrin and photosan are currently in clinical use for PDT of lung cancer.^{3,4} There is also considerable interest in understanding the factors contributing to the photodynamic activity of anthraquinones.^{5–7} The ability of some anthraquinone derivatives to form cytotoxic reactive oxygen species (ROS) after illumination can result in effective ablation of targeted tissue. However, anthraquinones often carry complications of systemic toxicity as they tend to both bind DNA^{8,9} and also cause

oxidative stress even without photoirradiation.¹⁰ Therefore, a prodrug of anthraquinone, which can be converted into anthraquinone only under photoirradiation, is required to overcome these disadvantages in cancer therapy. We have focused on the mechanism of photochemical degradation of 9-nitroanthracene to form anthraquinone via generation of nitric oxide (NO). A similar reaction is observed in 6-nitrobenzo[a]pyrene where the orientation of the nitro group is perpendicular to the aromatic ring due to the two protons located at the peri position, a similar situation for the nitro group in 9-nitroanthracene.¹¹ For 6-nitrobenzo[a]pyrene, three isomers of benzo[a]pyrenequinone are formed as a result of photodecomposition. If 9-nitroanthracene is used as a precursor of anthraquinone for PDT, complications of systemic toxicity can be avoided thereby benefiting its use in therapy. In this communication, we highlight a 9-nitroanthracene derivative (**1**) as a precursor of anthraquinone, an effective photosensitizer agent, and demonstrate its DNA cleaving activities under photoirradiation.

Keywords: Anthraquinone; 9-Nitroanthracene; Photodynamic therapy; DNA cleavage.

* Corresponding author. Tel.: +81 3 3700 1141; fax: +81 3 3707 6950; e-mail: fukuhara@nihs.go.jp

2. Results and discussion

For the purpose of PDT, **1** was designed to have a dimethyl aminoalkyl group at the 2-position of 9-nitroanthracene. This group should increase solubility and DNA-binding affinity compared to 9-nitroanthracene itself. The synthesis of **1** and its isomer (**2**) with a nitro group at the 1-position is described in Scheme 1. 2-Aminoanthracene was condensed with 4-dimethylaminobutyric acid to give the dimethylaminoalkyl derivative at 87% yield. Nitration of the derivative with HNO_3 in acetic anhydride proceeded at 1- and 9-positions to give compounds **2** and **1** at 25% and 58% yields, respectively.

Comparing the stabilities of **1** and **2** under photoirradiation, **1** was much more susceptible to decomposition than **2**, consistent with the fact that **1** is almost completely decomposed 3 hours later, while photodegradation of **2** is not observed under the same conditions as shown in Figure 1a. Product analysis after photolysis of **1** showed that anthraquinone derivative (AQ) was formed at 77% yield, the structure of which was confirmed by ^1H NMR and mass spectrometry. It is likely that photolabile **1** releases NO in the course of anthraquinone formation. To assess the generation of NO upon photoirradiation, an ESR experiment with (MGD)- Fe^{2+} as the spin trap¹² was performed. As shown in Figure 1b, a three-line spectrum consistent of $a^{\text{N}} = 1.25$ mT and $g^{\text{iso}} = 2.04$, characteristic of the $[(\text{MGD})_2\text{Fe}^{2+}\text{-NO}]$ complex, was observed from photoirradiated **1**, indicating that degradation of photolabile **1** is accompanied by generation of NO. In contrast, we could barely observe a similar peak in the case of photostable **2**. These results show that **1** is a promising photosensitizer that is converted into an AQ structure under photoirradiation via a NO-releasing mechanism.

Photosensitizers are activated by light to induce cell death or modulation of immunological cascades, presumably via formation of ROS. Therefore, the abilities of **1** and **2** to cleave DNA were examined by agarose gel electrophoresis of pBR322DNA. As shown in Figure 2a, no effect of **1** and **2** on DNA was observed in the dark condition. When irradiation was performed for 30 min, **1** induced efficient strand cleavage as shown in Figure 2b, and in the presence of 200 μM **1**, almost all

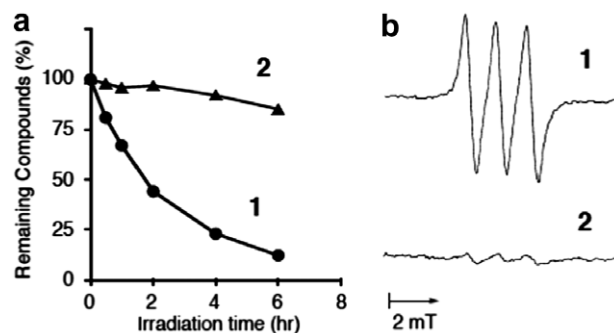


Figure 1. Photodegradation of **1** and **2**, and generation of NO. (a) Remaining **1** and **2** after photodegradation. (b) ESR spectra of (MGD)- Fe^{2+} in the presence of **1** and **2** after photoirradiation for 6 min.

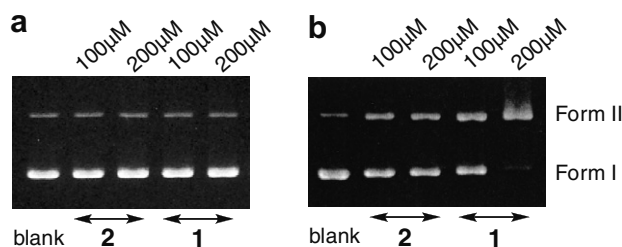
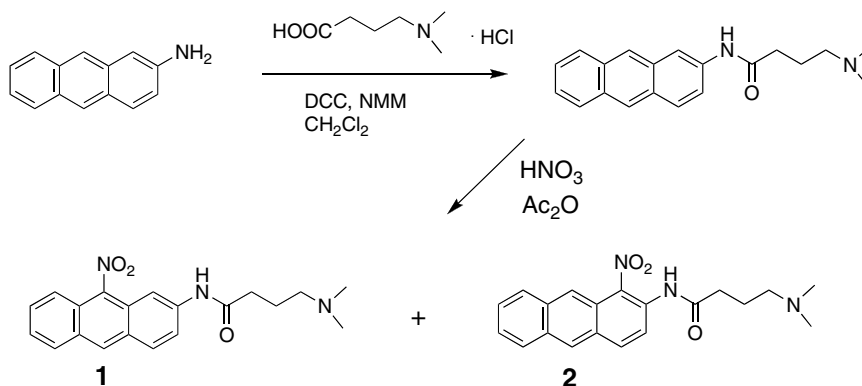


Figure 2. Effects of **1** and **2** on supercoiled pBR322DNA in the dark (a) or under photoirradiation (b).

of Form I (supercoiled) DNA was converted to Form II (closed circular) DNA. In contrast, although strand scission by **2** was obviously observed, the DNA-cleaving ability was not so strong compared with that of **1**. The strong DNA cleavage induced by **1** might be triggered by a structural change in AQ under photoirradiation. To confirm the generation of $^1\text{O}_2$ under photoirradiation, ESR spectra were observed in the presence of 2,2,6,6-tetramethyl-4-piperidone (4-oxo-TEMPO), a spin trap for $^1\text{O}_2$. As shown in Figure 3, a three-line spectrum consistent of $a^{\text{N}} = 1.60$ mT, which is characteristic of 4-oxo-TEMPO,¹³ was observed from both **1** and **2**, indicating generation of $^1\text{O}_2$. Importantly, the ability of **1** to generate $^1\text{O}_2$ as reflected in the peak height of 4-oxo-TEMPO was stronger than that for **2**, demonstrating



Scheme 1. Structures of **1** and **2**, and their synthesis.

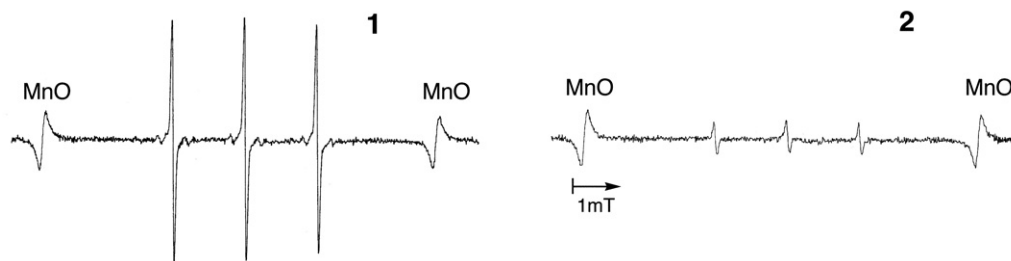


Figure 3. ESR spectra of 4-oxo-TEMP in the presence of **1** and **2** after photoirradiation for 10 min.

the advantage of **1** in cleaving DNA after conversion into AQ.

Photoexcited AQ (AQ^{3*}) is responsible for DNA damage through electron transfer from the DNA base (Type I mechanism)¹⁴ or by generation of ROS such as $^1\text{O}_2$ (Type II mechanism).¹⁵ Both mechanisms would result in DNA strand scission primarily at guanines. Therefore, photocleavage experiments induced by **1** were also performed with 5'- ^{32}P -end labeled oligonucleotides to test targeting of specific cleaving sites. As expected, irradiation of DNA in the presence of **1** for

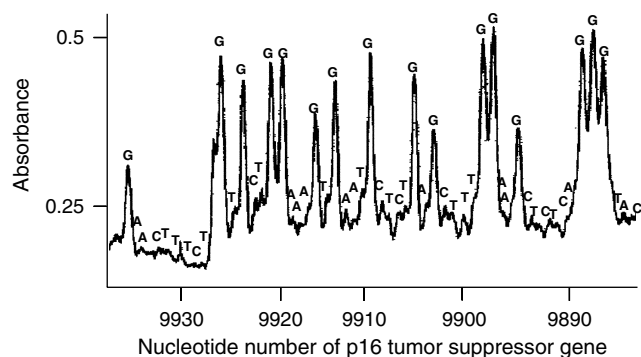
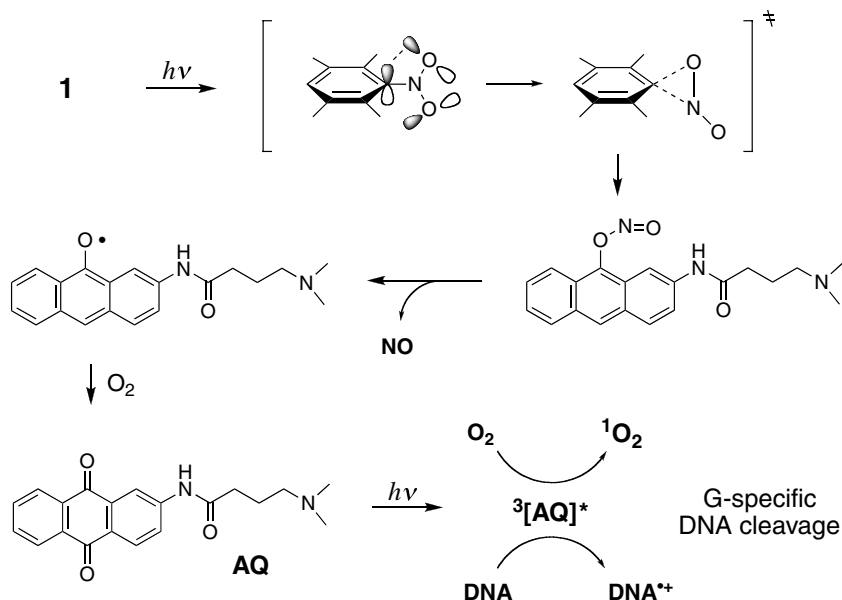


Figure 4. Sequence specificity of DNA damage in the p16 tumor suppressor gene, induced by **1** upon photoirradiation.

30 min and subsequent treatment with piperidine revealed that strand cleavage occurs predominantly at guanine, as shown in Figure 4.

In summary, we have described the design and synthesis of **1** as a precursor of anthraquinone, a typical photosensitizer. Photochemical conversion of **1** into anthraquinone via generation of NO and specific DNA cleavage at guanine were demonstrated, characteristic of DNA-cleaving reactions of anthraquinones. A possible mechanism of oxidative DNA cleavage induced by photoirradiated **1** is shown in Scheme 2. The perpendicular conformation of the nitro group to the anthracene is characteristic for **1** and is responsible for the ease of NO generation which is followed by structural conversion into anthraquinone.¹⁶ That is, the perpendicular conformation of nitro group in **1** suggests that the overlap of half-vacant nonbonding orbital of the nitro group with the adjacent orbital of the aromatic ring increases susceptibility to intramolecular rearrangement from nitro to nitrite. In comparison, such rearrangement does not occur in the case of **2** where the conformation of nitro group is not perpendicular (data not shown). There are a number of nitro polycyclic aromatic hydrocarbons (nitroPAHs) showing mutagenicity and/or carcinogenicity. However, no such toxicity has been shown by 9-nitroanthracene because the nitro group at 9-position is insensitive to enzymatic reduction, essential



Scheme 2. Possible mechanism of oxidative DNA damage induced by photoirradiated **1**.

for the toxicity of nitroPAH.¹⁷ Interestingly, two peri protons at the 1- and 8-positions, which lead to a perpendicular conformation of the nitro group, impede access of reductase to 9-nitroanthracene.^{17,18} Finally, **1** might be favorable for PDT as an approach to reducing the systemic toxicity of anthraquinone. Further investigation to understand the mechanism of DNA cleaving activity and apoptotic cell death induced by **1** is underway and will be reported in due course.

3. Experimental

3.1. General methods

The reagents and solvents used were of commercial origin (Wako chemicals, Sigma, Aldrich) and were employed without further purification. The progress of all reactions was monitored by thin-layer chromatography on silica gel 60 F₂₅₄ (0.25 mm, Merck). Column chromatography was performed on silica gel 60 (0.063–0.200 mm, Merck). The ¹H NMR spectra were recorded with a Varian AS 400 Mercury spectrometer. Chemical shifts were expressed in ppm downfield shift from Me₄Si. High resolution mass spectra were obtained on a JEOL MS700 mass spectrometer. ESR spectra were obtained with a JEOL X-band spectrometer (JES-FA100) under nonsaturating microwave power conditions.

3.2. Synthesis of *N*-(anthracen-2-yl)-4-(dimethylamino)butanamide (**3**)

To a solution of 2-aminoanthracene (580 mg, 3 mmol) and *N*-methylmorpholine (303 mg, 3 mmol) in DMF (10 ml) were added 4-(dimethylamino)butyric acid hydrochloride (503 mg, 3 mmol) and *N*-methylmorpholine (303 mg, 3 mmol) in DMF (10 ml) at 0 °C and the mixture was stirred for 18 h. After removal of the solvent in vacuo, the residue was dissolved in CH₂Cl₂ and filtered. The filtrate was washed with saturated NaCl, dried over anhydrous Na₂SO₄, and concentrated in vacuo. The residue was purified by silica gel column chromatography (CH₂Cl₂/MeOH/Satd NH₃ in MeOH, 100:20:1) to afford the title compound (796 mg, 87%) as a white solid. ¹HMR (CDCl₃, 400 MHz) δ 1.95 (2H, m), 2.40 (6H, s), 2.54 (2H, m), 2.61 (2H, m), 7.38 (1H, d, *J* = 9.2 Hz), 7.43 (2H, m), 7.94 (1H, d, *J* = 8.8 Hz), 7.95 (1H, d, *J* = 7.6 Hz), 7.96 (1H, d, *J* = 9.2 Hz), 8.34 (1H, s), 8.35 (1H, s), 8.47 (1H, s), 10.11 (1H, br); HR-MS (+EI) (M)⁺ found 306.1731; (M)⁺ calcd for C₂₀H₂₂N₂O 306.1734.

3.3. Synthesis of 4-(dimethylamino)-*N*-(9-nitroanthracen-2-yl)butanamide (**1**) and 4-(dimethylamino)-*N*-(1-nitroanthracen-2-yl)butanamide (**2**)

To a suspension of **1** (238 mg, 0.78 mmol) in acetic anhydride (35 mL) was added HNO₃ (0.17 mL) in acetic acid (1.8 mL) dropwise over 10 min at –10 °C. After stirring at 0 °C for 20 min, the mixture was poured onto crushed ice and stirred for 2 h, extracted with CH₂Cl₂, and the extracts were washed with H₂O and brine, dried

over anhydrous Na₂SO₄, and concentrated in vacuo. The residue was purified by silica gel column chromatography (benzene/ethyl acetate/MeOH/Satd NH₃ in MeOH, 40:40:15:5) to afford **2** and **1** in this order as a light orange solid.

1. 159 mg, 58% yield, UV λ_{max} (MeOH) nm: 224, 260, 364; ¹HMR (CDCl₃, 400 MHz) δ 1.93 (2H, m), 2.43 (6H, s), 2.57 (2H, m), 2.62 (2H, m), 7.51 (1H, m), 7.63 (1H, m), 7.89 (1H, s), 7.93 (1H, d, *J* = 8.8 Hz), 8.02 (1H, d, *J* = 9.1 Hz), 8.03 (1H, d, *J* = 8.4 Hz), 8.09 (1H, d, *J* = 9.1 Hz), 8.54 (1H, s), 11.22 (1H, br); HR-MS (+EI) (M)⁺ found 351.1585; (M)⁺ calcd for C₂₀H₂₁N₃O₃ 351.1584.

2. 68 mg, 25% yield, UV λ_{max} (MeOH) nm: 241, 269, 379; ¹HMR (CDCl₃, 400 MHz) δ 1.96 (2H, m), 2.32 (6H, s), 2.49 (2H, m), 2.61 (2H, m), 7.55 (2H, m), 8.01 (2H, m), 8.15 (1H, d, *J* = 9.4 Hz), 8.29 (1H, d, *J* = 9.4 Hz), 8.45 (1H, s), 8.62 (1H, s), 10.20 (1H, br); HR-MS (+EI) (M)⁺ found 351.1581; (M)⁺ calcd for C₂₀H₂₁N₃O₃ 351.1584.

3.4. Photolysis of **1**

A 3.5 mg (0.01 mmol) of **1** was dissolved in 4 ml of benzene/acetone (1:1) and irradiation was performed through a Pyrex filter with a 300W photoreactor lamp for 3 h. The reaction mixture was concentrated in vacuo and purified by silica gel column chromatography (benzene/ethyl acetate/MeOH/Satd NH₃ in MeOH, 40:45:10:5) to afford 4-(dimethylamino)-*N*-(9,10-dioxo-9,10-dihydroanthracen-2-yl)butanamide (AQ) as a pale yellow solid (2.6 mg, 77% yield). UV λ_{max} (MeOH) nm: 219, 272, 356; ¹HMR (CDCl₃, 400 MHz) δ 2.29 (2H, m), 2.89 (6H, s), 2.94 (2H, m), 3.18 (2H, m), 7.97 (2H, m), 8.10 (1H, d, *J* = 8.8 Hz), 8.21 (1H, d, *J* = .8 Hz), 8.26 (1H, d, *J* = 8.0 Hz), 8.29 (1H, d, *J* = 8.0 Hz), 8.61 (1H, s), 10.33 (1H, br); HR-MS (+EI) (M)⁺ found 336.1476; (M)⁺ calcd for C₂₀H₂₀N₂O₃ 336.1475.

3.5. Detection of nitric oxide and ¹O₂ by ESR

The Fe²⁺ complex of MGD [Fe²⁺-MGD₂, (Fe-MGD)] was used to trap NO. Fresh stock solutions of Fe-MGD (1:5) were prepared by adding ferrous ammonium sulfate to an aqueous solution of MGD. A sample containing 200 μM of **1** or **2** and 15 mM MGD-Fe in phosphate buffer, pH 7.6 (5% DMF) was introduced into a quartz flat cell. ESR spectra were recorded after light irradiation (5 J/cm² UVA) at 30 cm distance with a JES-FE 2XG spectrometer (JEOL Co. Ltd., Tokyo, Japan). The spectrometer settings used were: modulation frequency, 100 kHz; amplitude, 100–1000; scan time, 4 min; microwave power, 16 mW; microwave frequency, 9.394 GHz. Detection of ¹O₂ was performed by ESR using 2,2,6,6-tetramethyl-4-piperidone (4-oxo-TEMP) as a spin trap. A sample containing 100 μM of **1** or **2** and 100 mM of TEMP in phosphate buffer, pH 7.4 (5% DMF) was introduced into a quartz flat cell. ESR spectra were recorded in a similar manner as above.

3.6. Assays for DNA strand breaks

DNA strand breakage was measured by the conversion of supercoiled pBR322 plasmid DNA to the open circular form. Reactions were carried out in 20 μ L (total volume) of 50 mM Na cacodylate buffer (5% DMF), pH 7.2, containing 45 μ M of pBR322 DNA and 100 and 200 μ M of **1** and **2**. The mixture was exposed to 5 J/cm² UVA light on ice using a 10 W UV lamp (365 nm, UVP, Inc., CA, USA) placed at a distance of 20 cm. After 30 min, the reaction mixtures were treated with 5 μ L of loading buffer (100 mM TBE buffer, pH 8.3, containing 30% glycerol, 0.1% bromophenol blue) and applied to a 1% agarose gel. Horizontal gel electrophoresis was carried out in 50 mM TBE buffer, pH 8.3, and gels were stained with ethidium bromide (1 μ g/ml) for 30 min, followed by destaining in water for 30 min and photography with UV transillumination.

3.7. Site specificity of DNA damage induced by **1**

3.7.1. Preparation of ³²P-5'-end-labeled DNA fragments. DNA fragments were obtained from the human p16 tumor suppressor genes. The ³²P-3'-end-labeled 460-base pair fragment (*Eco*RI*9481–*Eco*RI*9940) containing exon 2 of the human p16 tumor suppressor gene was obtained as previously described.¹⁹ The 460-bp fragment was further digested with *Bss*HII to obtain the singly labeled 309-base pair (*Bss*HII 9789–*Eco*RI*9481) and 147-base pair (*Bss*HII*9794–*Eco*RI*9940) DNA fragments.²⁰ An asterisk indicates ³²P labeling.

3.7.2. Detection of DNA damage induced by UVA in the presence of **1.** The standard reaction mixture in a microtube (1.5-ml Eppendorf) contained a ³²P-labeled DNA fragment, 5 μ M calf thymus DNA, and **1** in 10 mM sodium phosphate buffer (pH 7.8) containing 5 μ M DTPA. The mixture was exposed to 5 J/cm² UVA light on ice using a 10 W UV lamp (365 nm, UVP, Inc., CA, USA) placed at a distance of 10 cm. After irradiation, the DNA fragments were treated for 20 min at 90 °C in 1 M piperidine and then electrophoresed on an 8% polyacrylamide/8 M urea gel. The autoradiogram was obtained by exposing an X-ray film to the gel. The preferred cleavage sites were determined by direct comparison of the position of the oligonucleotides with those produced by the chemical reactions of Maxam–Gilbert procedure using a DNA sequencing system (LKB2010 Macrophor). The relative amounts of oligonucleotides from treated DNA fragments were measured with a laser densitometer (LKB 2222 Ultrascan XL).

Acknowledgments

This work was supported partly by a Grant from the Ministry of Health, Labour and Welfare, and by a Grant-in-Aid for Research of Health Sciences focusing on Drug Innovation (KH51058) from the Japan Health Sciences Foundation, partly by Grant-in-Aid for Scientific Research (B) (No. 17390033) from the Ministry of Education, Culture, Sports, Science and Technology, Japan.

References and notes

1. Dougherty, T. J. *Photochemically Activated Anticancer Agents*; American Chemical Society: Washington, DC, 1995.
2. Dalla Via, L.; Marciari Magno, S. *Curr. Med. Chem.* **2001**, *8*, 1405–1418.
3. Fisher, A. M.; Murphree, A. L.; Gomer, C. J. *Lasers Surg. Med.* **1995**, *17*, 2–31.
4. Boyle, R. W.; Dolphin, D. *Photochem. Photobiol.* **1996**, *64*, 469–485.
5. Diwu, Z.; Lown, J. W. *Pharmacol. Ther.* **1994**, *63*, 1–35.
6. Andreoni, A.; Colasanti, A.; Malatesta, V.; Riccio, P.; Roberti, G. *Photochem. Photobiol.* **1991**, *53*, 797–805.
7. Johnson Inbaraj, J.; Krishna, M. C.; Gandhidasan, R.; Murugesan, R. *Biochim. Biophys. Acta* **1999**, *1472*, 462–470.
8. McKnight, R. E.; Zhang, J.; Dixon, D. W. *Bioorg. Med. Chem. Lett.* **2004**, *14*, 401–404.
9. Chou, K. M.; Krapcho, A. P.; Horn, D.; Hacker, M. *Biochem. Pharmacol.* **2002**, *63*, 1143–1147.
10. Venditti, P.; Balestrieri, M.; De Leo, T.; Di Meo, S. *Cardiovasc. Res.* **1998**, *38*, 695–702.
11. Fukuhara, K.; Kurihara, M.; Miyata, N. *J. Am. Chem. Soc.* **2001**, *123*, 8662–8666.
12. Komarov, A.; Mattson, D.; Jones, M. M.; Singh, P. K.; Lai, C. S. *Biochem. Biophys. Res. Commun.* **1993**, *195*, 1191–1198.
13. Moan, J.; Wold, E. *Nature* **1979**, *279*, 450–451.
14. Breslin, D. T.; Schuster, G. B. *J. Am. Chem. Soc.* **1996**, *118*, 2311–2319.
15. Reszka, K. J.; Bilski, P.; Chignell, C. F.; Hartley, J. A.; Khan, N.; Souhami, R. L.; Mendonca, A. J.; Lown, J. W. *J. Photochem. Photobiol. B* **1992**, *15*, 317–335.
16. Warner, S. D.; Farant, J. P.; Butler, I. S. *Chemosphere* **2004**, *54*, 1207–1215.
17. Fu, P. P.; Heflich, R. H.; Von Tungeln, L. S.; Yang, D. T.; Fifer, E. K.; Beland, F. A. *Carcinogenesis* **1986**, *7*, 1819–1827.
18. Miller, D. W.; Evans, F. E.; Fu, P. P. *Spectrosc. Int. J.* **1985**, *4*, 91–94.
19. Serrano, M.; Hannon, G. J.; Beach, D. *Nature* **1993**, *366*, 704–707.
20. Oikawa, S.; Hirosawa, I.; Hirakawa, K.; Kawanishi, S. *Carcinogenesis* **2001**, *22*, 1239–1245.